

This work was written as part of one of the author's official duties as an Employee of the United States Government and is therefore a work of the United States Government. In accordance with 17 U.S.C. 105, no copyright protection is available for such works under U.S. Law. Access to this work was provided by the University of Maryland, Baltimore County (UMBC) ScholarWorks@UMBC digital repository on the Maryland Shared Open Access (MD-SOAR) platform.

Please provide feedback

Please support the ScholarWorks@UMBC repository by emailing scholarworks-group@umbc.edu and telling us what having access to this work means to you and why it's important to you. Thank you.

PROCEEDINGS OF SPIE

[SPIDigitalLibrary.org/conference-proceedings-of-spie](https://www.spiedigitallibrary.org/conference-proceedings-of-spie)

Quasi-normal modes description of waves in 1-D photonic crystal

Severini, Sergio, Settimi, A., Mattiucci, N., Sibilia, Concita, Centini, Marco, et al.

Sergio Severini, A. Settimi, N. Mattiucci, Concita Sibilia, Marco Centini, Giuseppe D'Aguanno, Mario Bertolotti, Michael Scalora, Mark J. Bloemer, Charles M. Bowden, "Quasi-normal modes description of waves in 1-D photonic crystal," Proc. SPIE 5036, Photonics, Devices, and Systems II, (8 July 2003); doi: 10.1117/12.515402

SPIE.

Event: Photonics, Devices, and Systems II, 2002, Prague, Czech Republic

Quasi Normal Modes description of waves in 1-D photonic crystal

S. Severini^{*a}, A. Settimi^a, N. Mattiucci^a, C. Sibilìa^{**a}, M. Centini^a, G. D'Aguanno^a, M. Bertolotti^a,
M. Scalora^b, M. Bloemer^b, C.M. Bowden^b

^aINFM at Dipartimento di Energetica – Università “La Sapienza” di Roma – Via A. Scarpa 16, 00161 Roma, Italy; ^bWeapons Sciences Directorate, AMSMI-RD-WS-ST, RD & EC, US Army Missile Command, Building 7804, Redstone Arsenal, AL 35898-5000, USA

ABSTRACT

For the first time the quasi normal mode treatment is used and extended to the description of the scalar field behaviour in one dimensional photonic crystals. A one-dimensional photonic crystal is a particular configuration of an open cavity, where discontinuities into refractive index give rise to field confinement. A discussion of the complex eigenvalues and eigenfrequencies, as well as the corresponding field distribution, is presented.

Keywords: photonic band gap structures, quasi normal modes description, optical cavity, open systems

1. INTRODUCTION

In this work, we adopt a description of the scalar field in 1-D PC in terms of “Quasi Normal Modes”. The description of the e.m. field in an optical cavity in terms of “Quasi Normal Modes” has been discussed for example by Ching¹ et al. Because of the “leakage”, the “modes” of the cavity are quasinormal modes (QNM), characterized by complex frequencies. In Ching's paper¹, QNM's are discussed in a one dimensional leaky cavity, provided the cavity is defined by a discontinuity in the refractive index which must approach its constant asymptotic value sufficiently rapidly.

2. NORMAL AND QUASI NORMAL MODES

The QNM treatment presents formal analogies with the treatment of hermitian systems. The main analogy is the form of solutions of equation

$$\left[\rho(x) \frac{\partial^2}{\partial t^2} - \frac{\partial^2}{\partial x^2} \right] E(x, t) = 0 \quad (1.1.)$$

$$\rho(x) = \left(\frac{n(x)}{c} \right)^2 \quad (1.2.)$$

given as $E_j(x, t) = f_j(x) \exp(-i\omega_j t)$ but where ω_j are complex frequencies. The ordinary theory of normal modes gives the general solution of eq. (1.1.), as a summation of a numerable (but discrete) number of terms of the kind:

$$E_n(x, t) = f_n(x) e^{-i\omega_n t} \quad (1.3.)$$

* sergio.severini@uniroma1.it; phone +39 06 4991 6942; fax +39 06 4424 0183; <http://www.uniroma1.it>; Dipartimento di Energetica, Via Scarpa 16, 00161 Roma, Italy;

** concita.sibilìa@uniroma1.it; phone +39 06 4991 6541; fax +39 06 4424 0183; <http://www.uniroma1.it>; Dipartimento di Energetica, Via Scarpa 16, 00161 Roma, Italy;

where $n = \pm 1, \pm 2, \dots$ and for perfectly closed cavity from $x = 0$ to $x = a$ (normal modes) we require that

$$f_n(0) = 0 \quad (1.4.)$$

$$f_n(a) = 0 \quad (1.5.)$$

If we arrange all the eigenvalues, in crescent order $0 < \omega_1 \leq \omega_2 \leq \dots$, we have:

$$\omega_{-n} = -\omega_n \quad (1.6.)$$

$$f_{-n}(x) = f_n(x) \quad (1.7.)$$

With respect to the inner product

$$\langle \phi | \psi \rangle = \int dx \phi^*(x) \rho(x) \psi(x) \quad (1.8.)$$

the eigenfunctions $f_n(x)$ form an orthogonal base: in this case we talk of normal modes (NMs). For one side open cavity, the structure of solutions (1.3.) remains the same. If we put eq. (1.3.) into eq. (1.1.) we obtain the following eigenvalues equation

$$H f_n(x) = \omega_n^2 f_n(x) \quad (1.9.)$$

where H is an operator defined as $H = -\rho^{-1}(x) \partial_x^2$. Because energy is not bounded inside the cavity, there is an exchange of energy between the cavity and the external bath. Outside the cavity (for $x \geq a$) the field $E(x, t)$ is an outgoing wave $E(x - ct)$. The “outgoing wave” condition makes the Hamilton operator (1.9.) not hermitian inside the cavity. Frequencies ω_n become complex, with $\text{Im}(\omega_n) < 0$, and from the observation of eq. (1.3.) it is evident that modes are not stationary. With the exception of zero modes, i.e. modes for which we have $\text{Re}(\omega_0) = 0$, all the other modes satisfy the following conditions²:

$$\omega_{-n} = -\omega_n^* \quad (1.10.)$$

$$f_{-n}(x) = f_n^*(x) \quad (1.11.)$$

where we have preventively arranged all the eigenvalues so that $0 < \text{Re}(\omega_1) \leq \text{Re}(\omega_2) \leq \dots$.

Since $\omega_{-n}^2 \neq \omega_n^2$, eigenfunctions $f_n(x)$ and $f_{-n}(x)$ are linearly independent. As we will see in the next section, this representation is complete, inside the cavity only. This kind of representation takes the name of Quasi Normal Modes.

3. QNMs for generic open cavities

We first consider optical cavities open from one side. In these structures we try to find solutions of equation (1.1.) using the Green function formalism³, considering that at one side of the cavity there is a perfect mirror. We consider the causal Green function, defined as

$$\left[\rho(x) \frac{\partial^2}{\partial t^2} - \frac{\partial^2}{\partial x^2} \right] G(x, y; t) = \delta(t) \delta(x - y) \quad (3.1.)$$

and the following initial conditions:

$$\begin{aligned} G(x, y; t) &= 0, \quad t \leq 0 \\ \rho(x) \frac{\partial G(x, y; t)}{\partial t} \Big|_{t=0^+} &= \delta(x - y) \end{aligned} \quad (3.2.)$$

The Fourier transform $\tilde{G}(x, y; \omega)$ of the Green function satisfies the following equation:

$$\left[\frac{\partial^2}{\partial x^2} + \omega^2 \rho(x) \right] \tilde{G}(x, y; \omega) = -\delta(x - y) \quad (3.3.)$$

We introduce two auxiliary functions $g_{\pm}(x, \omega)$, solutions of the homogeneous equation:

$$\left[\frac{\partial^2}{\partial x^2} + \omega^2 \rho(x) \right] g_{\pm}(x, \omega) = 0 \quad (3.4.)$$

with the following conditions:

$$g_{-}(x=0, \omega) = 0 \quad (3.5.)$$

$$g_{+}(x, \omega) = \exp(i\omega x/c) \quad (3.6.)$$

for $x \rightarrow \infty$.

The Wronskian associated to the two homogeneous equations for $g_{\pm}(x, \omega)$ is x -independent, so we have:

$$W(\omega) = g_{+}(x, \omega)g'_{-}(x, \omega) - g_{-}(x, \omega)g'_{+}(x, \omega) \quad (3.7.)$$

One may demonstrate that⁴:

$$\tilde{G}(x, y; \omega) = \begin{cases} -\frac{g_{-}(x, \omega)g_{+}(y, \omega)}{W(\omega)}, & \text{for } 0 < x < y \\ -\frac{g_{+}(x, \omega)g_{-}(y, \omega)}{W(\omega)}, & \text{for } 0 < y < x \end{cases} \quad (3.8.)$$

The QNMs correspond to all the poles of $\tilde{G}(x, y; \omega)$. From the previous condition it follows that QNMs correspond to all the zeroes of $W(\omega)$. Residues of $\tilde{G}(x, y; \omega)$, in the poles $\omega = \omega_n$, are given by⁴:

$$R_n = -\frac{g_{-}(x, \omega_n)g_{+}(x, \omega_n)}{\left. \frac{dW}{d\omega} \right|_{\omega=\omega_n}} \quad (3.9.)$$

The Green function we are searching for $t \geq 0$, is the inverse Fourier transform of $\tilde{G}(x, y; \omega)$

$$G(x, y; t) = \frac{1}{2\pi} \oint \tilde{G}(x, y; \omega) e^{i\omega t} d\omega \quad (3.10.)$$

In this anti-transformation we work with complex values of the saturated dynamical variable ω . There are three contributions to the entire integral⁵ (3.10.):

- a) “*instantaneous response*”: it is due to the summation of $\tilde{G}(x, y; \omega)$ on the semi-infinite circumference, linked to the transitory time,
- b) “*retarded response*”: it is due to long time contributions,
- c) “*intermediary response*”: this contribution gives rise to the oscillations of the QNMs, for intermediary time and it is due to the zeros of the Wronskian.

If we apply the WKB² approximation, in order to study $\tilde{G}(x, y; \omega)$ for $|\omega| \rightarrow \infty$, under suitable hypothesis⁶, we have

$$\tilde{G}(x, y; \omega) \cong \frac{\sin[\omega I(0, y)] [e^{-i\omega I(x, a)} + \text{Re}^{i\omega I(x, a)}]}{\omega \sqrt{n(x)n(y)} [e^{-i\omega I(0, a)} + \text{Re}^{i\omega I(0, a)}]} \quad (3.11.)$$

where we have introduced:

$$I(u, v) = \int_u^v \rho(x) dx \quad (3.12.)$$

that is positive for $v > u$. In the hypothesis of $\omega = \omega_R + i\omega_I \rightarrow \infty$, with $\omega_I < 0$, we have:

$$\tilde{G}(x, y; \omega) \cong \frac{e^{|\omega_I| I(0, y)} e^{|\omega_I| I(x, a)}}{\omega e^{|\omega_I| I(0, a)}} \quad (3.13.)$$

If $y \leq x$, because of $I(0, y) + I(x, a) \leq I(0, a)$, $\tilde{G}(x, y; \omega)$ goes to zero if $|\omega| \rightarrow \infty$ with $\omega_I < 0$; if $x, y > a$, $\tilde{G}(x, y; \omega)$ can not satisfy the same condition. We can conclude saying that only inside the cavity the QNMs representation is complete.

4. QNMS FOR PBG STRUCTURES.

PBG is a both side open cavity. A PBG is a particular structure in which we have a refractive index of the kind

$$n(x) = \begin{cases} n_0(x) & , \text{ for } x < x_0 \\ n_j(x) & , \text{ for } x_{j-1} < x < x_j, \text{ where } j \in [1, N] \\ n_{N+1}(x) & , \text{ for } x > x_N \end{cases} \quad (4.1.)$$

that is continuous at intervals, as depicted in the following figure 1.

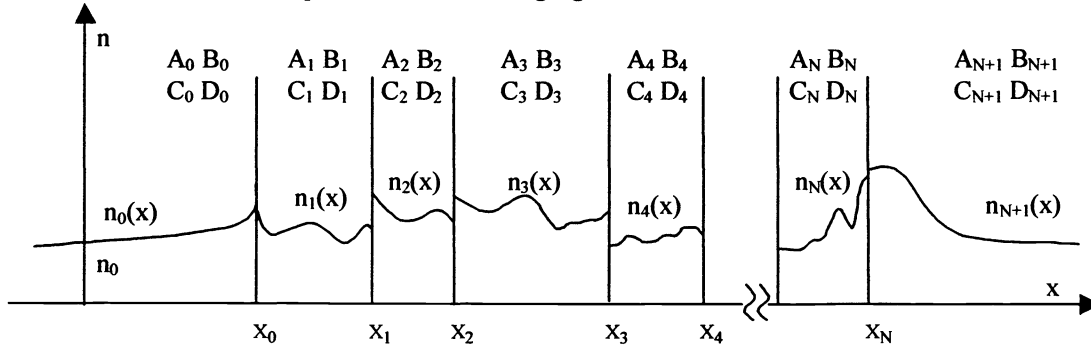


Figure 1: Representation of the refractive index spatial distribution. x is the longitudinal propagation chord. In each interval, refractive index is constant.

We suppose that

$$\lim_{x \rightarrow -\infty} n_0(x) = \lim_{x \rightarrow \infty} n_{N+1}(x) = n_0 \quad (4.2.)$$

i.e. outside the PBG structure there is a homogeneous isotropic medium with a constant refractive index. For a PBG we have a cavity, in a space $I=[0, a]$, that is coupled with a bath $I' = (-\infty, 0) \cup (a, +\infty)$. For normal incidence of the fields, the structure of the field equation is the same as eq. (1.1.). The two auxiliary functions $g_{\pm}(x, \omega)$ satisfy equation (3.4.) with the following boundary conditions:

$$g_+(x, \omega) = e^{i n_0 \frac{\omega}{c} x}, \text{ for } x \rightarrow +\infty \quad (4.3.)$$

$$g_-(x, \omega) = e^{-i n_0 \frac{\omega}{c} x}, \text{ for } x \rightarrow -\infty \quad (4.4.)$$

Using the WKB method for the Green function at high frequencies ($|\omega| \rightarrow \infty$), we obtain for the auxiliary function $g_{\pm}(x, \omega)$:

$$\begin{cases} g_-(x, \omega) = A_j(\omega) e^{i \frac{\omega}{c} \int_x^{x_j} n(\xi) d\xi} + B_j(\omega) e^{-i \frac{\omega}{c} \int_x^{x_j} n(\xi) d\xi} & x_{j-1} < x < x_j \\ g_-(x, \omega) = e^{-i \frac{\omega}{c} \int_x^{x_0} n(\xi) d\xi} & x < x_0 \end{cases} \quad (4.5.)$$

where $j \in [1, N+1]$ and $x_{N+1} = +\infty$. For the auxiliary function $g_+(x, \omega)$ we have:

$$\begin{cases} g_+(x, \omega) = C_j(\omega) e^{i \frac{\omega}{c} \int_{x_{j-1}}^x n(\xi) d\xi} + D_j(\omega) e^{-i \frac{\omega}{c} \int_{x_{j-1}}^x n(\xi) d\xi} & x_{j-1} < x < x_j \\ g_+(x, \omega) = e^{i \frac{\omega}{c} \int_{x_N}^x n(\xi) d\xi} & x > x_N \end{cases} \quad (4.6.)$$

where $j \in [0, N]$ and $x_{-1} = -\infty$. Therefore $\forall (x, y) | x_0 < y \leq x < x_N \Rightarrow \exists k | x_0 < y \leq x_k, x_{k-1} \leq x < x_N$. For $k \leq m \leq N$ and $1 \leq n \leq k$ we obtain⁶ for the Green function (for $y \leq x$) the following expression:

$$\tilde{G}(x, y; \omega) = - \frac{\begin{bmatrix} A_n(\omega) e^{i \frac{\omega}{c} \int_y^{x_n} n(\xi) d\xi} + B_n(\omega) e^{-i \frac{\omega}{c} \int_y^{x_n} n(\xi) d\xi} \\ C_m(\omega) e^{i \frac{\omega}{c} \int_{x_{m-1}}^x n(\xi) d\xi} + D_m(\omega) e^{-i \frac{\omega}{c} \int_{x_{m-1}}^x n(\xi) d\xi} \end{bmatrix}}{2i \frac{\omega}{c} n(x) \begin{bmatrix} D_m(\omega) B_n(\omega) e^{-i \frac{\omega}{c} \int_{x_{m-1}}^{x_n} n(\xi) d\xi} \\ -C_m(\omega) A_n(\omega) e^{i \frac{\omega}{c} \int_{x_{m-1}}^{x_n} n(\xi) d\xi} \end{bmatrix}} \quad (4.7.)$$

where the coefficients in the previous formula are given from the boundary conditions in $x = x_j$. If we take into consideration the dominant coefficients only⁶, equation (4.7.) becomes:

$$\tilde{G}(x, y, \omega) \cong - \frac{e^{-i \frac{\omega}{c} \left[\int_y^{x_0} n(\xi) d\xi + \int_{x_{m-1}}^x n(\xi) d\xi \right]}}{2i \frac{\omega}{c} n(x) e^{-i \frac{\omega}{c} \int_{x_{m-1}}^{x_0} n(\xi) d\xi}} \quad (4.8.)$$

Since for $y \leq x$ we have:

$$\int_y^{x_n} n(\xi) d\xi + \int_{x_{m-1}}^x n(\xi) d\xi = \int_{x_{m-1}}^{x_n} n(\xi) d\xi + \int_y^{x_{m-1}} n(\xi) d\xi \leq \int_{x_{m-1}}^{x_n} n(\xi) d\xi \quad (4.9.)$$

the Green function in a PBG structure has the following behaviour:

$$\tilde{G}(x, y, \omega) \rightarrow 0 \text{ for } |\omega| \rightarrow \infty \quad (4.10.)$$

The convergence condition is satisfied, so we can conclude that the QNMs representation is complete inside the PBG structure.

5. QNM frequencies and functions for PBG structures.

The calculation of the QNM eigenfrequencies is based on the matrix methods⁷. This method uses the Chebyshev polynomial functions. In order to obtain conditions (4.3.)–(4.4.) for $g_{\pm}(x, \omega)$, the following conditions $A_0(\omega_n) = 0$, and $D_{N+1}(\omega_n) = 0$, are valid in equations (4.5.)–(4.6.).

We divide the entire space x into $2N+3$ regions in each of which the index of refraction $n(x)$ is constant. For a generic interval (x_{j-1}, x_j) , with $j = 0, 1, \dots, 2N+1, 2N+2$ and $x_{-1} = -\infty$ and $x_{2N+1} = \infty$, the index of refraction takes the constant value n_j :

$$n_j = \begin{cases} 1 & , \text{ for } j = 0, 2N+2 \\ n_h & , \text{ for } j = 1, 3, \dots, 2N-1, 2N+1 \\ n_l & , \text{ for } j = 2, 4, \dots, 2N \end{cases} \quad (5.1.)$$

as schematically depicted in figure 2.

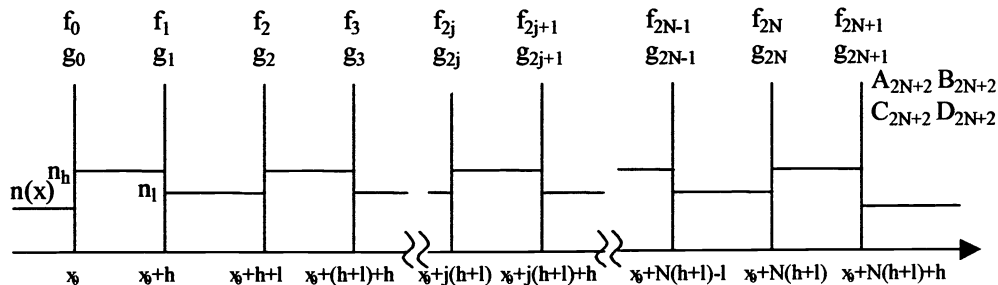


Figure 2: Typical behaviour of the refractive index in a PBG structure. For each region n is constant.

If we introduce the two phase-terms

$$\begin{cases} \delta_l = q_l l = n_l l \frac{\omega}{c} \\ \delta_h = q_h h = n_h h \frac{\omega}{c} \end{cases} \quad (5.2.)$$

the QNM-frequencies can be found by solving the following transcendental equation, with real coefficients:

$$\alpha \sum_{j=0}^{\left[\frac{N-1}{2}\right]} \frac{(-1)^j (N-1-j)!}{j! (N-1-2j)!} (\gamma)^{N-1-2j} + \beta \sum_{j=0}^{\left[\frac{N-2}{2}\right]} \frac{(-1)^j (N-2-j)!}{j! (N-2-2j)!} (\gamma)^{N-2-2j} = 0 \quad (5.3.)$$

where α , β and γ are particular functions⁶ of n_h and n_l .

Equation (5.3.) depends only on PBG parameters. If we work with a quarter-wave PBG, equation (5.3.) becomes a real coefficients polynomial equation (instead of a transcendental equation) of degree $N(m_l + m_h) + m_h$ in the variable $e^{2i\delta}$. The QNM-functions can be constructed from⁶:

$$\begin{aligned} f(x) = & \left(A_0 e^{i\frac{\omega}{c}x} + B_0 e^{-i\frac{\omega}{c}x} \right) \mathcal{G}(-x) + \\ & + \sum_{j=0}^N \left(A_{2j+1} e^{i\frac{\omega}{c}n_h x} + B_{2j+1} e^{-i\frac{\omega}{c}n_h x} \right) \mathcal{G}(x - j(h+l)) \mathcal{G}(j(h+l) + \\ & + \sum_{j=0}^{N-1} \left(A_{2j+2} e^{i\frac{\omega}{c}n_l x} + B_{2j+2} e^{-i\frac{\omega}{c}n_l x} \right) \mathcal{G}(x - j(h+l) - h) \mathcal{G}((j+1)(h+l) - x) + \\ & + \left(A_{2N+2} e^{i\frac{\omega}{c}x} + B_{2N+2} e^{-i\frac{\omega}{c}x} \right) \mathcal{G}(x - N(h+l) - h) \end{aligned} \quad (5.4.)$$

where $\mathcal{G}(x)$ is the unitary step function. In figures 3 to 5 are printed some examples of positions of the QNM (complex) frequencies.

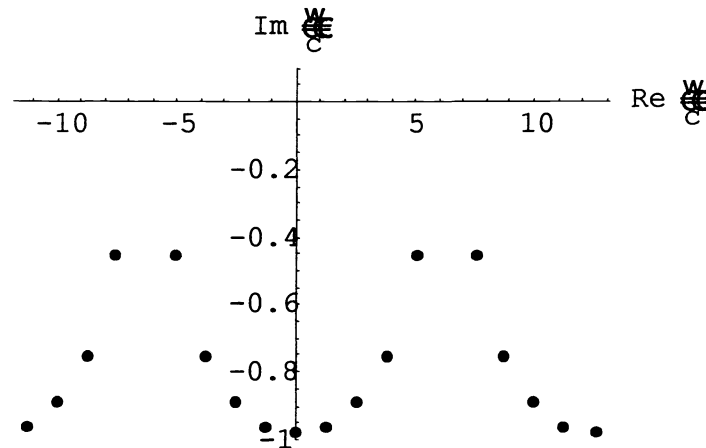


Figure 3: QNM-frequencies (complex) distribution for a PBG with $N=4$ and $n_h=1.41$, $n_l=1$.

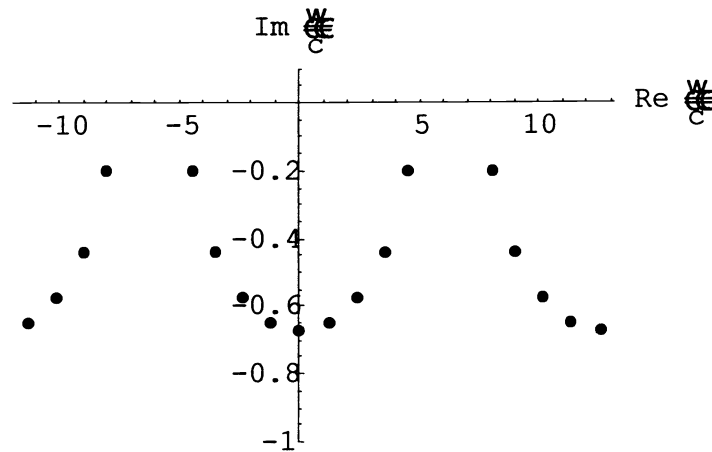


Figure 4: QNM-frequencies (complex) distribution for a PBG with $N=4$ and $n_h=2$, $n_l=1$

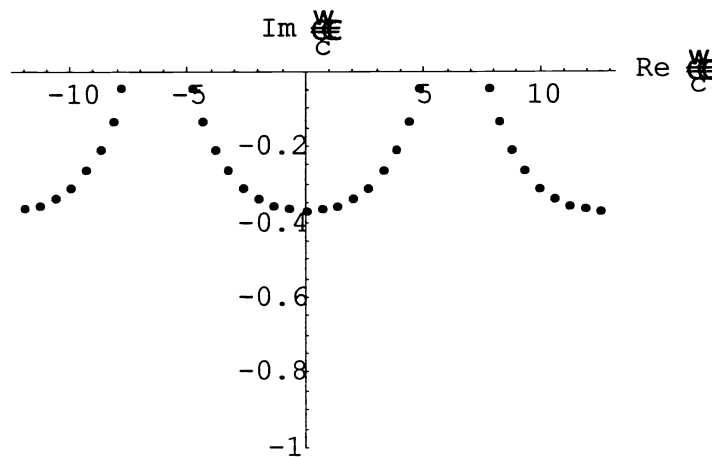


Figure 5: QNM-frequencies (complex) distribution for a PBG with $N=8$ and $n_h=2$, $n_l=1$.

From the observation of figures 3-4 we can see that the imaginary parts of the QNM's become larger when the refractive index leap decrease, for a fixed number of cells. In figures 4 and 5 it is evident the decreasing of the imaginary parts of the QNM frequencies for a doubling of the number of cells.

6. QNMS, EXAMPLES AND CONCLUSIONS

The n^{th} QNM frequency ω_n well describes the n^{th} transmission peak in the sense that: 1) $\text{Re}(\omega_n)$ is the resonance frequency of the n^{th} transmission peak; 2) $|\text{Im}(\omega_n)|$ is linked to the FWHM of the n^{th} transmission peak. It is relevant to point out that the eigenfunction $f_n(z)$ associated to the n^{th} QNM, of eigenfrequency ω_n , is such that the square modulus $|f_n(z)|^2$ give the amplitude field distribution inside the PBG structure at the frequency $\text{Re}(\omega_n)$.

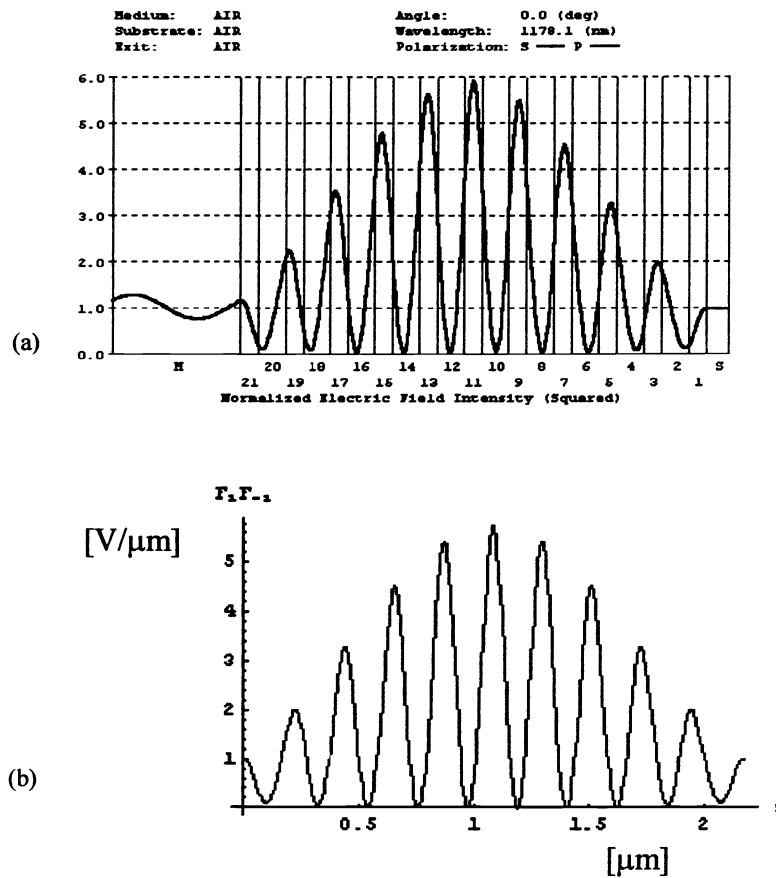


Figure 6: In (a) is printed the square modulus of the electric field inside the PBG structure calculated at $\lambda=1178$ nm. by numerical method based on the transmission matrix. In (b) is reported the square modulus of the QNM function associated to the same wavelength.

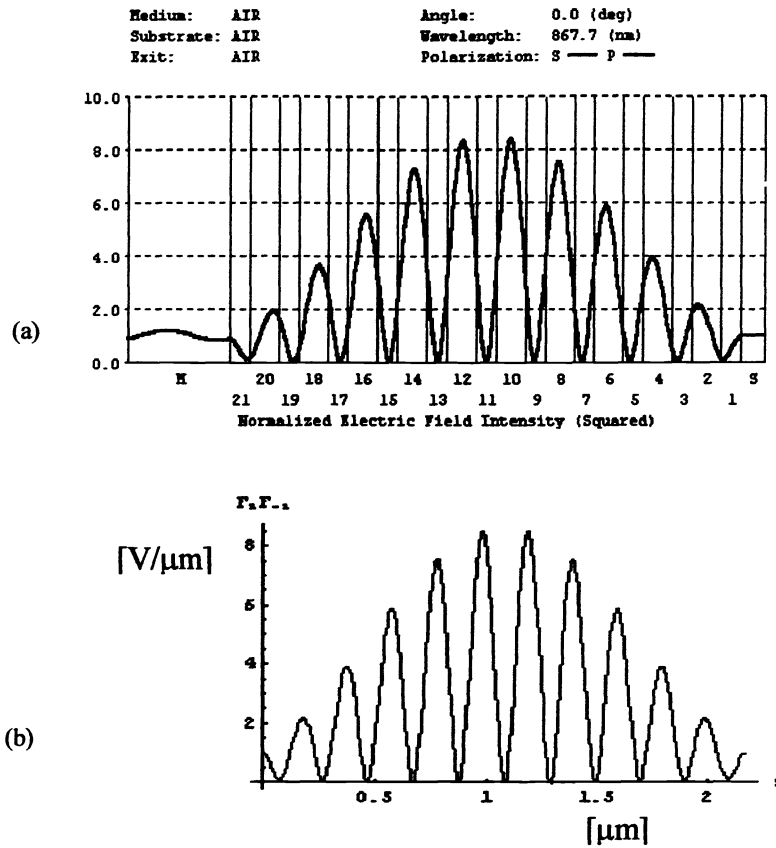


Figure 7: In (a) is printed the square modulus of the electric field inside the PBG structure calculated at $\lambda=867.7$ nm by numerical method based on the transmission matrix. In (b) is reported the square modulus of the QNM function associated to the same wavelength.

In figs. 6a, 7a and 8a are reported the field distributions calculated with numerical scattering methods; in figs. 6b, 7b and 8b the corresponding distributions are calculated with the QNM theory. All the figures are evaluated for a PBG structure with $N=10$, $n_h=3$ and $n_l=2$. Comparing all the figures it is evident the coincidence between the QNM theory and numerical methods based on the transmission matrix⁷.

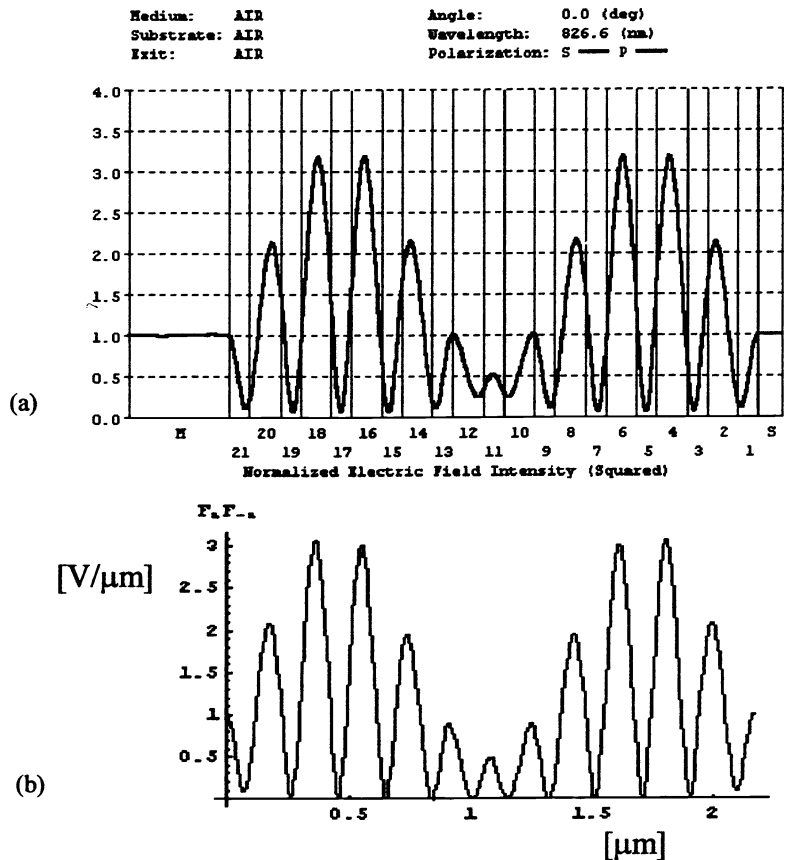


Figure 8: In (a) is printed the square modulus of the electric field inside the PBG structure calculated at $\lambda=826.6$ nm by numerical method based on the transmission matrix. In (b) is reported the square modulus of the QNM function associated to the same wavelength

REFERENCES

1. E. S. C. Ching, P. T. Leung, A. Maassen van der Brink, W. M. Suen, S. S. Tong, and K. Young, Rev. Mod. Phys. vol. 70, 1545-1554 (1998)
2. P. T. Leung, W. M. Suen, C. P. Sun and K. Young, Phys. Rev. E, vol. 57, pp. 6101-6104 (1998).
3. E.N. Economou, "Green's functions in Quantum Physics", Springer-Verlag (1979).
4. P.T. Leung, S.Y. Liu and K. Young, Phys. Rev. A, vol 49, 3057-3067 (1994).
5. E. S. C. Ching, P. T. Leung, A. Maassen van der Brink, W. M. Suen, S. S. Tong, and K. Young, Rev. Mod. Phys. vol. 70, 1545-1554 (1998).
6. S. Severini, A. Settini, N. Mattiucci, C. Sibilia, M. Centini, D'Aguzzo, M. Bertolotti, M. Scalora, M. Bloemer, C.M. Bowden "Quasi normal modes description of waves in 1-D photonic crystal », submitted to physical Review E.
7. J. Lenker, *Theory of reflection*, Martinus Nijhoff, Dordrecht, (1987).